J|A|C|S
COMMUNICATIONS

Published on Web 02/17/2007

Automated Spectral Compression for Fast Multidimensional NMR and Increased Time Resolution in Real-Time NMR Spectroscopy

Ewen Lescop, Paul Schanda, Rodolfo Rasia, and Bernhard Brutscher*

IBS, Institut de Biologie Structurale Jean-Pierre Ebel, 41 rue Jules Horowitz, F-38027 Grenoble; CEA; CNRS; UJF

Received December 14, 2006; E-mail: bernhard.brutscher@ibs.fr

Multidimensional (nD) NMR spectroscopy is a versatile tool for the study of molecular structure, dynamics, and kinetics in solution. In an ideal NMR experiment, each correlation peak reports on the physicochemical properties of the molecular environment at the site of a nuclear spin. For larger molecules, or molecules with a low chemical shift dispersion, an increasing number of spins needs to be correlated in a single 2D, 3D, 4D, or higher-dimensional spectrum to solve the NMR overlap problem. A major drawback of nD NMR is the increase in experimental time by about 2 orders of magnitude for each additional dimension. In protein NMR, the acquisition time of many common experiments exceeds the time required to achieve a sufficient signal-to-noise ratio. To make nD NMR more time-efficient, alternative sampling schemes are required that allow free adjustment of the acquisition time to the intrinsic sensitivity of the experimental setup (sample, spectrometer, pulse sequence). Many elegant approaches for fast data acquisition have been proposed recently, for example, nonlinear data sampling, projection NMR, Hadamard spectroscopy, spatial frequency encoding,[1] and fast-pulsing techniques.[2] Here we present automated spectral compression (ASCOM), a complementary fast NMR technique that exploits available knowledge from prior collected data to increase the peak density in spectral space without loss of information. We demonstrate the use of ASCOM for the study of molecular kinetics based on a series of ^{1}H$-^{15}$N correlation spectra recorded at 1 s^{-1} rates and for chemical shift assignment using 4D experiments that can be performed in a few hours.

In Fourier-transform (FT) NMR, the choice of the spectral width SW determines the number of (complex) data points n to be recorded to achieve a given spectral resolution $\Delta\nu$ via the relation $n = \mathrm{SW}/\Delta\nu$. A reduced spectral width results in fewer repetitions of the pulse sequence and thus in shorter experimental times. If SW is chosen smaller than the chemical shift range of the observed nuclear spins, this results in spectral aliasing (folding). Resonance frequency offsets ν_0 outside the chosen spectral width give rise to NMR signals at $\nu = \epsilon^k\,[\nu_0 - k\ \mathrm{sign}(\nu_0)\mathrm{SW}]$ depending whether the time domain data are complex ($\epsilon = 1$) or real ($\epsilon = -1$). The variable k is the number of times the peak has been aliased. To avoid accidental peak overlap, spectral aliasing is generally kept to a minimum. If the chemical shifts of one or several nuclear spin species are already known from previously recorded spectra, this information can be exploited to minimize SW for further data acquisition involving the same nuclear spins. For example, ^{1}H$-^{15}$N and ^{1}H$-^{13}$C correlation experiments are generally performed during the early stage of an NMR protein study. We have developed a simple algorithm that optimizes $\mathrm{SW_X}$ (X = ^{15}N or ^{13}C) based on the (^{1}H, X) peak list of a protein (ASCOM-1). Spectra are calculated for each $\mathrm{SW_X}$ by representing the cross-peaks by ellipses defined by line width parameters in the two dimensions (Supporting Information, Figure S2). The number of resolved cross-peaks is computed as a function of $\mathrm{SW_X}$. Here we focus on complex data as obtained from STATES,[3a] STATES-TPPI,[3b] or echo/antiecho[3c] quadrature detection. For complex NMR data, the ASCOM optimization is independent of the X carrier frequency and thus requires less computation. Fast computation becomes important when using ASCOM directly on the NMR spectrometer for automated optimization of acquisition parameters. Figure 1a shows that, for small to medium sized proteins, high degrees of compression with minimal or no loss of spectral information are achieved from ASCOM-1 optimization of the ^{15}N spectral width. ^{1}H$-^{15}$N spectra recorded for ubiquitin using $\mathrm{SW_N}$ = 25 ppm (85 resolved peaks) and $\mathrm{SW_N}$ = 5.7 ppm (81 resolved peaks) are shown in Figure 1b.

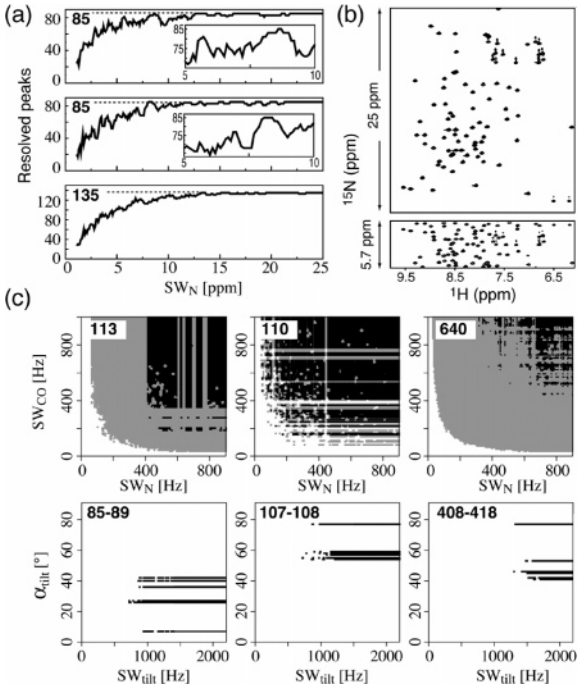

Figure 1. (a) ASCOM-1 optimization of $\mathrm{SW_N}$ ($\mathbf{B}_0$ = 18.8 T, $\Delta\nu_H = \Delta\nu_N$ = 30 Hz) for ^{1}H$-^{15}$N correlation experiments of different proteins: 76-residue ubiquitin (top), a 103-residue fragment of Hyl1 (Hyl1-1)[4] (center), and 147-residue WZB (bottom, BMRB 6934). ASCOM-1 is particularly attractive for small proteins with a low intrinsic peak density. (b) Ubiquitin ^{1}H$-^{15}$N correlation spectra recorded for different ^{15}N spectral widths. (c) ASCOM-2$_{SW}$ (top) and ASCOM-2$_{proj}$ (bottom) optimizations assuming $\mathbf{B}_0$ = 14.1 T, $\Delta\nu_H$ = 30 Hz, $\Delta\nu_N = \Delta\nu_{CO}$ = 15 Hz. Results are shown for the natively unstructured γ-synuclein (left, BMRB 7244), Hyl1-1 (center), and malate synthase G (right, BMRB 5471). In ASCOM-2$_{proj}$ a peak is counted as resolved if it does not overlap in at least one of the two projections. Parameter combinations for which a maximum of cross-peaks (number given in the upper left corner) are resolved are color-coded in black. The additional gray surface areas indicate the ASCOM-2$_{SW}$ results for a number of resolved cross-peaks equal to the maximum obtained by ASCOM-2$_{proj}$. For smaller proteins, the two approaches yield comparable results. For large or unstructured protein, only ASCOM-2$_{SW}$ resolves all possible peaks while providing significant data compression.

As a first application of interest, a series of SOFAST-HMQC ^{1}H$-^{15}$N spectra[2a] can be recorded with a repetition rate of ~1 spectrum/second to follow a kinetic process in real time. So far,

10.1021/ja068949u CCC: $37.00

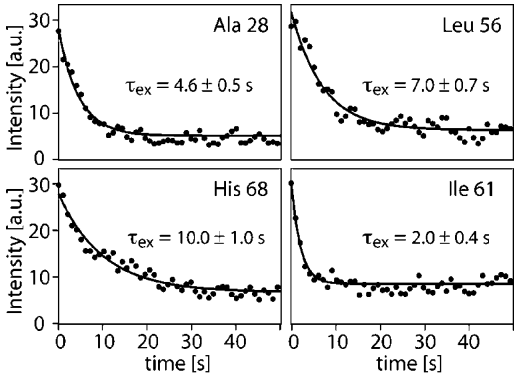

Figure 2. H/D exchange rates measured for amide sites in ubiquitin (1.4 mM, pH 10.8, 2 M urea, 25 °C, 18.8 T). The exchange reaction was initiated by fast injection[2e] of a 50 μL protein−H_2O solution into 350 μL of D_2O. The dead time of the experiment was ∼2 s. The ASCOM-1 optimized ^{15}N spectral width for this sample (48 cross-peaks observable) was 4.9 ppm. SOFAST-HMQC[2a] spectra were recorded with eight complex points in t_1 (5 ms recycle delay) in an overall time of 1 s.

the time resolution of 2D real-time protein NMR has been limited to ∼5 s using standard SOFAST-HMQC. Hadamard-encoded SOFAST-HMQC[2b] or spatially encoded ultraSOFAST HMQC[2c] also yield 1 s^{-1} repetition rates, but the former focuses on a set of selected amide sites, and the latter requires very high protein concentrations. ASCOM-optimized SOFAST-HMQC yields 1 s time resolution simultaneously for all amide sites resolved in the ^{1}H−^{15}N correlation map using moderate protein concentrations. To illustrate this method, we have measured fast amide hydrogen−deuterium exchange in ubiquitin under weak denaturing conditions at high pH. The H/D exchange rates measured under such conditions provide useful information on global unfolding events in the protein.[5] Representative examples of exchange curves are shown in Figure 2. These results clearly demonstrate that real-time 2D NMR measurements of kinetic events down to characteristic time constants τ_{ex} of a few seconds are accessible to ASCOM-1 optimized SOFAST-HMQC. Other interesting applications of ASCOM-1 comprise ^{15}N relaxation measurements, ^{13}C, ^{15}N-edited 3D and 4D ^{1}H−^{1}H NOESY, and 3D H−N−X correlation experiments as required for resonance assignment.

The ASCOM approach can be extended to 3-dimensional spectral space if chemical shift information for three correlated nuclei is available. In ASCOM-2, two spectral parameters are optimized simultaneously, either (i) the spectral widths in the two indirect dimensions (ASCOM-2_{SW}) or (ii) a tilt angle and a tilted spectral width for recording a pair of plane projections (ASCOM-2_{proj}).[6] Here, we focus on correlation experiments required for protein resonance assignment. Recording of 4D NMR spectra with high resolution generally requires unreasonably long acquisition times of >1 week. Therefore, resonance assignment is usually performed based on a set of 3D spectra. With ASCOM-2, however, recording of 4D H−N−CO−X spectra becomes possible in an experimental time comparable to a 3D experiment. The peak density is optimized on the basis of the correlated frequency information obtained from a prior recorded 3D H−N−CO data set. The small number of HNCO peaks (about one per residue), makes ASCOM-2 an efficient tool. For small proteins, ASCOM-2_{proj} yields highest data compression, while still resolving most of the correlation peaks. For larger or unstructured proteins, however, fewer peaks are resolved in the ASCOM-2_{proj}-optimized projections than in the 3D spectrum, as illustrated in Figure 1c.

Even for the 723-residue MSG protein, ASCOM-2_{SW} yields optimized ^{15}N, ^{13}CO spectral widths of only ∼500 Hz.

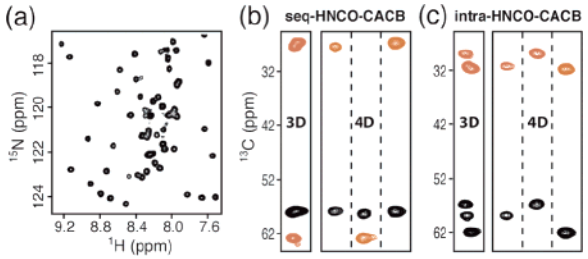

Figure 3. (a) Central part of a ^{1}H−^{15}N HSQC spectrum of Hyl1-1. (b, c) 2D ^{1}H−^{13}C strips extracted from 3D and 4D seq-HNCO-CACB and intra-HNCO-CACB spectra at ω_H = 8.2 ppm, ω_N = 122.2 ppm, and ω_{CO} = 174.6, 175.0, and 179.7 ppm for the 4D data sets. The 4D spectra shown in panels b and c were recorded at 600 MHz on a 0.4 mM sample in an experimental time of 20 and 40 h, respectively, using ASCOM-2_{SW} optimized ^{15}N and ^{13}CO spectral widths of 141 and 483 Hz, respectively.

Figure 3 shows 2D strips extracted from ASCOM-2_{SW} optimized sequential and intraresidue 4D HNCO-CACB experiments (Figure S5) of Hyl1-1. These experiments provide chemical shift information for five nuclei in a single data set. The 4D spectra solve ambiguities remaining in a 3D spectrum because of overlapping ^{1}H−^{15}N correlations, by dispersing the peaks along an additional CO dimension. Therefore they greatly facilitate spectral analysis and sequential assignment, especially for the crowded central spectral regions. By combining ASCOM-2 optimization with the BEST concept,[2d] introduced recently for fast pulsing NMR, a complete 4D HNCO-CACB data set can be recorded in less than 4 h as long as sensitivity is not the limiting factor. This is demonstrated for a 2 mM sample of ubiquitin in Supporting Information Figure S6.

In summary, we have introduced ASCOM a simple tool that optimizes the peak density in 2D or 3D spectral space in order to reduce data acquisition times. We expect that this approach will prove very useful for the study of larger molecular systems, unfolded or partially folded proteins using higher-dimensional NMR, as well as for the study of unidirectional biophysical processes by real-time 2D NMR spectroscopy.

Acknowledgment. We thank J. Boisbouvier (IBS) for making the Hyl1-1 sample available and A. Favier (IBS) for implementing ASCOM on Varian spectrometers.

Supporting Information Available: Further details on the ASCOM algorithm, BEST HNCO-CACB pulse sequences, and ASCOM-optimized 4D spectra of ubiquitin. This material is available free of charge via the Internet at http://pubs.acs.org.

References

(1) (a) Reviewed in Freeman, R.; Kupce, E. *J. Biomol. NMR* **2003**, *27*, 101−113. (b) Malmodulin, D.; Billeter, M. *Prog. Nucl. Magn. Reson. Spectrosc.* **2005**, *46*, 109−129.
(2) (a) Schanda, P.; Brutscher, B. *J. Am. Chem. Soc.* **2005**, *127*, 8014−8015. Schanda, P.; Kupce, E.; Brutscher B. *J. Biomol. NMR* **2005**, *33*, 199−211. (b) Schanda, P.; Brutscher, B. *J. Magn. Reson.* **2006**, *178*, 334−339. (c) Gal, M.; Schanda, P.; Brutscher B.; Frydman, L. *J. Am. Chem. Soc.* **2007**, *129*, 1372−1377. (d) Schanda, P.; Van Melckebeke, H.; Brutscher, B. *J. Am. Chem. Soc.* **2006**, *128*, 9042−9043. (e) Mok, K. H.; Nagashima, T.; Day, I. J.; Jones, J. A.; Jones, C. J. V.; Dobson, C. V.; Hore, P. J. *J. Am. Chem. Soc.* **2003**, *125*, 12484−12492.
(3) (a) States, D. J.; Haberkorn, R. A.; Ruben, D. J. *J. Magn. Reson.* **1982**, *48*, 286−292. (b) Marion, D.; Ikura, M.; Tschudin, R.; Bax, A. *J. Magn. Reson.* **1989**, *85*, 393−399. (c) Palmer, A. G.; Cavanagh, J.; Wright, P. E.; Rance, M. *J. Magn. Reson.* **1994**, *93*, 151−170.
(4) Han, M. H.; Goud, S.; Song, L.; Fedoroff, N. *Proc. Natl. Acad. Sci. U.S.A.* **2004**, *101*, 1093−1098.
(5) Dempsey, C. E. *Prog. Nucl. Magn. Reson. Spectrosc.* **2001**, *39*, 135−170. Ferraro, D. M.; Lazo, N. D.; Robertson, A. *Biochemistry* **2004**, *43*, 587−594.
(6) Tugarinov, V.; Choy, W.-Y.; Kupce, E.; Kay, L. E. *J. Biomol. NMR* **2004**, *30*, 347−352.

JA068949U